Colloid Polym Sci (2009) 287:847–851
DOI 10.1007/s00396-009-2039-7

ORIGINAL CONTRIBUTION

Synthesis and characterization of silver—poly(methylmethacrylate) nanocomposites

Vesna V. Vodnik · Jasna V. Vuković · Jovan M. Nedeljković

Received: 28 January 2009 / Revised: 31 March 2009 / Accepted: 9 April 2009 / Published online: 29 April 2009

Abstract The optical properties of silver nanoparticles embedded in poly(methylmethacrylate) (PMMA) was investigated as well as the influence of silver nanoparticles on the thermal properties of polymer matrix. The average size and particle size distribution of silver nanoparticles was determined using transmission electron microscopy. The obtained transparent nanocomposite films were optically characterized using UV-Vis and FTIR spectroscopy. Thermal stability of polymer matrix was improved upon incorporation of small amount of silver nanoparticles. Also, silver nanoparticles have pronounced effect on thermooxidative stability of PMMA matrix. The glass transition temperatures of nanocomposites are lower compared to the pure polymer.

Keywords Silver nanoparticles · PMMA · Nanocomposite · Thermal stability · Glass transition temperature

Introduction

Incorporation of inorganic nanoparticles in a polymer matrix can significantly affect the properties of the matrix [1, 2]. The obtained nanocomposites might exhibit improved optical, thermal, mechanical, electrical, magnetic, and flammability properties. The properties of polymer composites depend on type of incorporated nanoparticles, their size and shape, their concentration and interaction with polymer matrix.

Noble metal particles such as silver and gold are of great significance due to their size-dependent optical properties [3–5]. Moreover, it was confirmed that antibacterial performance of silver nanoparticles encapsulated in polymer matrix are still preserved according to efficiently suppress bacteria's growth including *Salmonella*, *Staphylococcus*, and *Escherichia coli* [6–8].

Many different synthetic procedures for preparation of Ag/PMMA composites are presented in literature: "core shell" synthesis [9, 10], ion implantation [11, 12], vapor phase co-deposition in vacuum [13], and suspension polymerization [14]. The main problem in polymer nanocomposite technology is the prevention of particle aggregation. This problem can be overcome by modification of the surface of the particles. The modification improves the interfacial interaction between the inorganic particles and the polymer matrix [1, 15, 16]. In this study, we used simple procedure for preparation of Ag/PMMA nanocomposites with homogeneous distribution of metal nanoparticles in the polymer matrix. Highly uniform Ag nanoparticles synthesized in water were surface-modified and by phase transfer process extracted into nonpolar organic solvent. In the second step, Ag nanoparticles were combined with commercial PMMA polymer dissolved in chloroform and, finally, after solvent evaporation transparent nanocomposite films were obtained. Microstructural characterization of Ag nanoparticles was performed by transmission electron microscopy. On the other hand, influence of Ag nanoparticles on the glass transition temperature, as well as on the thermal and thermooxidative stability of the PMMA matrix was studied in detail using

V. V. Vodnik · J. M. Nedeljković (✉)
Vinča Institute of Nuclear Sciences,
P.O. Box 522, 11001 Belgrade, Serbia
e-mail: jovned@vinca.rs

J. V. Vuković
Institute of Chemistry,
Technology and Metallurgy - Department of Chemistry,
University of Belgrade,
Njegoševa 12,
Belgrade, Serbia

differential scanning calorimetry (DSC) and thermogravimetry (TG).

Experimental

Materials

Silver nitrate ($AgNO_3$), sodium borohydride ($NaBH_4$), oleylamine, and chloroform were purchased from Merck. PMMA DIAKON^{TM} CMG 314V, synthesized via radical polymerization (M_w=9,0000 g/mol, M_w/M_n=2.195), was obtained from Lucite International. All the reagents were of analytical grade and used as received, without further purification. Milli-Q deionized water was used for synthesis.

Preparation of Ag/PMMA Nanocomposites

Silver hydrosols were prepared using $NaBH_4$ as a reducing agent, as described elsewhere [17]. Silver nanoparticles were transferred into organic solvent (chloroform) using oleylamine as transfer agent. Typically, 250 ml of aqueous colloidal solution of silver nanoparticles (5×10^{-4}M) was mixed with 25 ml of chloroform containing 1.52×10^{-2}M oleylamine. Almost instantaneous phase transfer was indicated with dark yellow color of organic phase divided from colorless aqueous phase. In order to prepare Ag/PMMA nanocomposites, silver nanoparticles dispersed in chloroform were mixed in an appropriate ratio with PMMA dissolved in chloroform. After evaporation of the solvent in vacuum oven at room temperature, yellow-colored transparent films with thickness of about 25 μm were obtained.

Apparatus

UV-Vis absorption spectra of silver nanoparticles in water and chloroform, as well as Ag/PMMA nanocomposite films were measured using Perkin-Elmer Lambda 5 spectrophotometer.

The size distribution of silver nanoparticles was determined using a PHILIPS EM-400 transmission electron microscope (TEM) operating at 100 kV. Samples for TEM measurements were prepared by placing a droplet of silver colloid onto a C-coated Cu grid and evaporating solvent.

IR measurements of pure PMMA and Ag/PMMA nanocomposites were carried out on a Bruker Vector 22 Spectrometer (Opus 2.2 Software).

Thermogravimetric analyses (TGA) were carried out on a Perkin Elmer TGS-2 instrument either in air or under nitrogen atmosphere (flow rate 25 cm^3/min) with heating rate of 10 °C/min.

Differential scanning calorimetry (DSC) measurements were performed using Perkin Elmer DSC-2 instrument in the temperature range from 50 °C to 170 °C under nitrogen atmosphere (heating rate was 20 °C/min).

Results and discussion

The absorption spectra of silver nanoparticles in water and chloroform are shown in Fig. 1 (curves a and b). The surface plasmon resonance band of silver nanoparticles in chloroform (peak position 407 nm) is red shifted for about 20 nm compared to the position of plasmon band of the initial water colloid. According to Drude model [4, 5], a red shift of the plasmon resonance frequency is expected by increasing the dielectric constant of the surrounding media (refractive indexes of water and chloroform are 1.333 and 1.445, respectively). No other changes were noticed in the absorption spectrum after phase transfer of silver nanoparticles from water to chloroform. Narrow half-width of surface plasmon absorption band (about 60 nm) indicated uniform size distribution of silver particles.

The average diameter and size distribution of silver nanoparticles in chloroform were determined using TEM. Typical TEM image and histogram of the size distribution are shown in Fig. 2. The average diameter of spherical silver nanoparticles was found to be 5.6 nm. Large areas of spontaneous organization of silver nanoparticles in the hexagonal, close-packed, 2D ordered arrangement could be detected easily, indicating the high mono-dispersity. The silver nanoparticles, although closely packed, are well separated due to the presence of the oleylamine layer, adsorbed on particle surface.

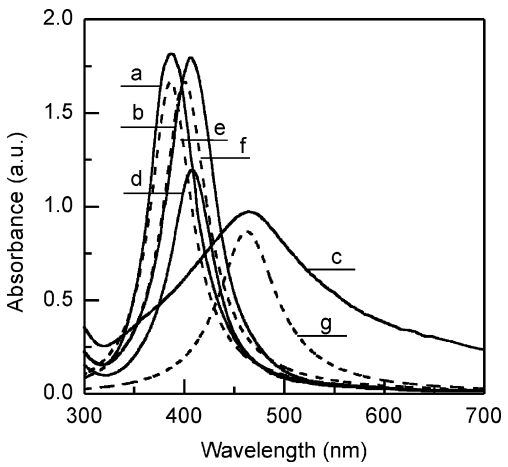

Fig. 1 UV-Vis absorption spectra of silver nanoparticles in *a* water, *b* chloroform, and *c* PMMA matrix, as well as *d* dissolved Ag/PMMA nanocomposite in chloroform. *e* Theoretical bands of silver nanoparticles in water and *f* chloroform, as well as of *g* Ag/PMMA nanocomposite obtained according to Maxwell–Garnett theory

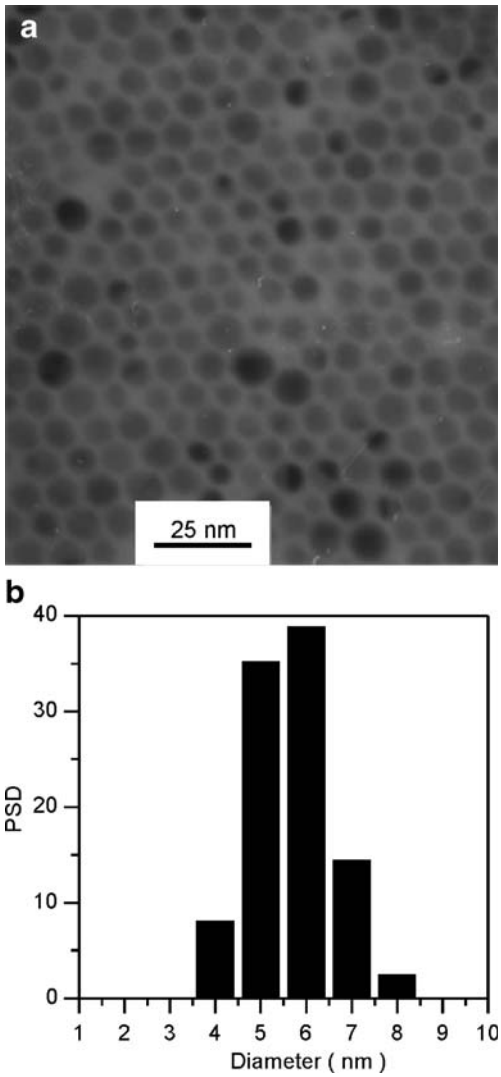

Fig. 2 Typical TEM image (**a**) and size distribution (**b**) of silver nanoparticles in chloroform

Absorption spectrum of silver nanoparticles embedded in PMMA matrix is shown in Fig. 1 (curve c). Significant red shift and broadening of surface plasmon absorption band upon incorporation of silver nanoparticles into PMMA matrix was observed compared to silver hydrosol or organosol. In order to exclude the possibility that observed changes are consequence of agglomeration of silver nanoparticles upon incorporation into polymer matrix, nanocomposite film was dissolved in chloroform, and absorption spectrum was compared with the initial absorption spectrum of silver nanoparticles in chloroform. Absorption spectrum of dissolved Ag/PMMA nanocomposite in chloroform (Fig. 1, curve d) was almost identical to the absorption spectrum of silver nanoparticles in chloroform after phase transfer from water (Fig. 1, curve b) indicating that incorporation process of silver nanoparticles into PMMA did not induce their agglomeration or growth.

In the Ag/PMMA nanocomposite film, the distances between the silver nanoparticles are smaller compared to those in the aqueous or chloroform solution. With the decrease of separation distances, the interaction between neighboring nanoparticles increases, and this additional energy shifts the surface plasmon resonance. The peak positions in the absorption spectra of the silver nanoparticles in aqueous and chloroform solution as well as in Ag/PMMA nanocomposite were reconstructed using well-known effective medium Maxwell–Garnett theory [18]; the theoretical bands are presented in Fig. 1 (curves e, f, and g, respectively). It was concluded for the Ag/PMMA film that the main contribution to the experimental spectrum arises for nanocomposite configuration with filling factor f=0.3, e.g., in the case of close-packed Ag nanoparticles, with interparticle distances of 2 nm. On the other hand, the calculated bands corresponding to the absorption spectra of silver in water and chloroform obtained for vanishing filling factors ($f \rightarrow 0$) show peak positions very similar to those obtained experimentally. The values for dielectric constants of water, chloroform, and PMMA used in the calculations were 1.778, 2.088, and 2.24, respectively.

In order to determine if chemical bonding between silver nanoparticles and the PMMA matrix had taken place, IR measurements were performed. No difference between the IR spectra of the pure PMMA and Ag/PMMA nanocomposites were found (IR spectra are not shown). These results indicate that Ag/PMMA nanocomposites resemble solid solution with weak interaction between the polymer matrix and nanofiller particles.

Thermal stability in nitrogen and air atmosphere of Ag/PMMA nanocomposite films was compared to the thermal stability of pure PMMA. TG and DTG curves obtained in nitrogen atmosphere for pure commercial PMMA and Ag/PMMA nanocomposites are shown in Fig. 3. The thermal degradation process of radically prepared PMMA has been a subject of numerous studies [19–24] and usually involves multiple steps assigned to: presence of relatively week head-to-head linkage, the scission of unsaturated end groups, and to the random scission. It is generally considered that most PMMA thermally degrade through depolymerization; therefore, the kinetics of mass loss are determined by the mode of depolymerization initiation.

The DTG curve of commercial PMMA shown in Fig. 3b have strong peak at 376 °C, suggesting that random chain scission is the main step during the polymer degradation process. With an increase of silver loading, the midpoint temperature is shifted toward higher values. For example, in the case of Ag/PMMA nanocomposite with 2 wt.% of inorganic phase, the thermal degradation is shifted toward higher temperatures for 26 °C indicating its better thermal stability compared to pure PMMA.

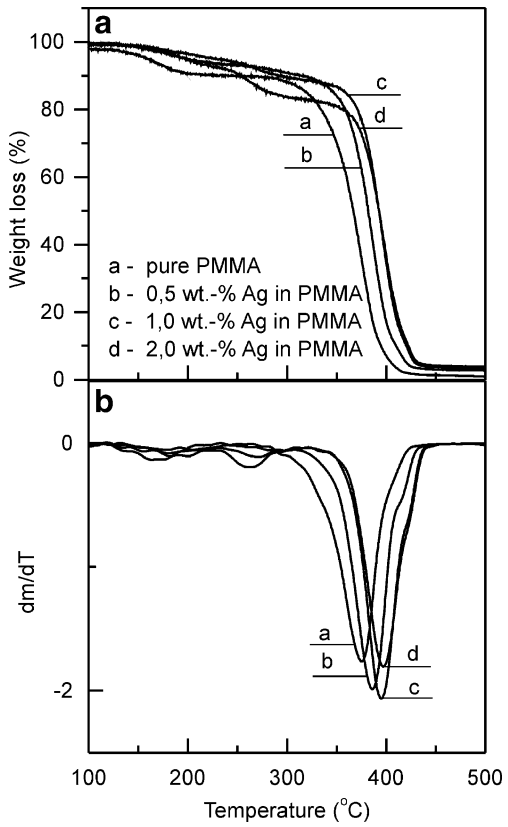

Fig. 3 TG (**a**) and DTG (**b**) curves of pure PMMA and Ag/PMMA nanocomposites with different content of inorganic phase, obtained in nitrogen atmosphere

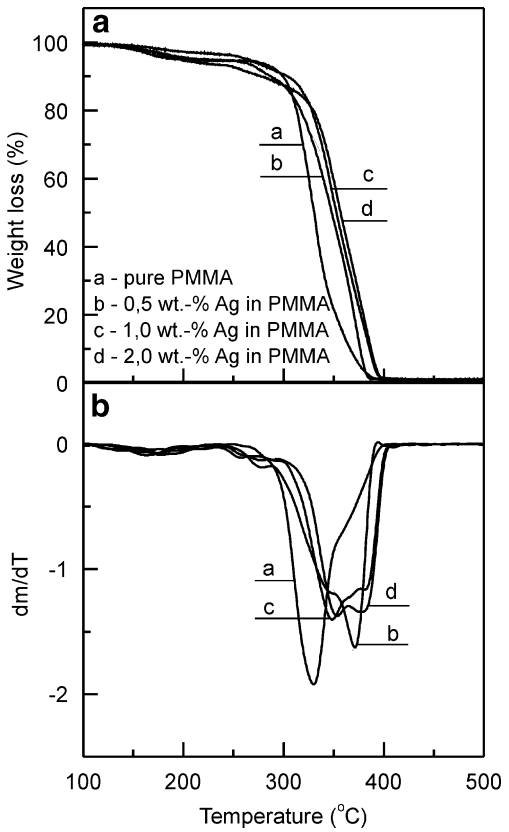

Fig. 4 TG (**a**) and DTG (**b**) curves of pure PMMA and Ag/PMMA nanocomposites with different content of inorganic phase, obtained in air

Most likely, the initial small peak at 167 °C originates from impurities in commercial sample of PMMA. On the other hand, DTG curves of Ag/PMMA nanocomposite films have one additional peak at 265 °C. The magnitude of this peak slightly increases with the increase of the content of inorganic phase. Marning et al. [25] have shown that the unsaturated ends are responsible for two weight loss stages around 180 °C and 270 °C. In this case, the degradation would be preferentially initiated by radical transfer to the vinyl chain end, i.e., by any reaction that generates a radical able to degrade the polymer by chain-transfer process. The sources of free radicals could be: impurities, H–H bonds, scission β to the vinyl group at unsaturated ends, and/or random scission. Based on these facts, we assigned small DTG peak observed at 265 °C to the degradation process initiated by radical transfer to unsaturated ends. It is possible that the silver nanoparticles itself might be a source which generates radicals.

The TG and DTG curves, obtained in air, are shown in Fig. 4. The mechanism of thermo-oxidative degradation of PMMA is more complex than that in nitrogen. The DTG curve of pure PMMA has peak and shoulder at 329 °C and 370 °C, respectively. This behavior can be explained by the dual function of oxygen in PMMA degradation. At lower temperatures, oxygen inhibits PMMA degradation by reacting with a polymeric radical and forming a stable peroxy radical. At higher temperatures (above 270 °C), peroxy radical degrades and releases a more reactive radical resulting in the acceleration of PMMA decomposition [26]. Under these conditions, the peak corresponding to the week head-to-head linkage (100–200 °C) disappears, and the peak that belongs to the scission of unsaturated end groups (200–300 °C) merges with the random scission peak at 300–400 °C. The thermo-oxidative stability of the PMMA matrix was much more influenced by the presence of the silver nanoparticles than its internal thermal stability. Incorporation of silver nanoparticles shifted the decomposition toward higher temperatures and led to the decrease of

Table 1 Glass transition temperature (T_g) of Ag/PMMA nanocomposites

Content of Ag in PMMA (wt.%)	T_g (°C)
0	97
0.5	96
1.0	92
2.0	91

the magnitude of the first DTG peak as well as to the transformation of DTG shoulder into well-resolved intense peak. The observed behavior is most likely a consequence of the inhibiting effects of the silver nanoparticles on some degradation stages of the thermo-oxidative degradation of PMMA.

The influence of silver nanoparticles on the glass transition behavior of polymer matrix was studied with dynamic DSC technique. The values of T_g were taken as the midpoint of the glass transition event and collected in Table 1. The pure commercial PMMA has a T_g value of 97 °C, while tendency of slight decrease of T_g values by increasing silver content was observed for Ag/PMMA nanocomposites. Generally, acording to literature, interaction of polymer chains with surface of nanoparticles can alter the chain kinetics decreasing [27–29] or increasing [30–32] glass transition temperature of the polymer. Ash et al. [27] explained the decrease of T_g values in terms of thin film model. When the interparticle distance is small enough (<10 nm), then the polymer between two particles can be considered as a thin film. As pointed out earlier in the part concerning calculation of optical spectra based on Maxwell–Garnett theory, interparticle distance was estimated to be 2 nm. Assuming that little or no interfacial interaction between the filler and matrix exists, the T_g decreases as the film thickness, i.e., interparticle distance decreases. This is consistent with observed influence of silver content on the T_g.

Acknowledgements This work was financially supported by the Ministry of Science and Technological Development of the Republic of Serbia (research project number: 142066). Also, the authors are grateful to Dušan Božanić for help in performing theoretical calculations.

References

1. Kickelbick G (2003) Prog Polym Sci 28:83
2. Caseri W (2000) Macromol Rapid Commun 21:705
3. Kelly KL, Coronado E, Zhao LL, Schatz GC (2003) J Phys Chem B 107:668
4. Mulvaney P (1996) Langmuir 12:788
5. Kreibig U, Vollmer M (1995) Optical properties of metal clusters. Springer Series in Material Science, No. 25, Springer-Verlag Berlin, p 26
6. Aymonier C, Schlotterbeck U, Antonetti L, Zacharias P, Thomann R, Tiller JC, Mecking S (2002) Chemm Commun 3018
7. Liedberg H, Lundeberg T (1987) Urol Res 17:357
8. Weickmann H, Tiller JC, Thomann R, Mulhaupt R (2005) Macromol Mater Eng 290:875
9. Wang L, Chen D (2004) Chem Lett 33:1010
10. Quaroni L, Chumanov G (1999) J Am Chem Soc 121:10642
11. Bazarov VV, Petukhov VY, Zhikharev VA, Khaibullin IB (1995) Mater Res Soc Sym Proc 388:417
12. Stepanov AL, Abdullin SN, Petukhov VY, Osin YN, Khaibullin RI, Khaibullin IB (2000) Philos Mag B 80:23
13. Takele H, Greve H, Pochstein C, Zaporojtchenko V, Faupel F (2006) Nanotechnology 17:3499
14. Yeum YH, Deng Y (2005) Colloid Polym Sci 283:1172
15. Marutani E, Yamamoto S, Ninjbagar T, Tsujii Y, Fukuda T, Takano M (2004) Polymer 45:2231
16. Zhang SW, Zhou SX, Weng YM, Wu LM (2005) Langmuir 21:2124
17. Vukovic VV, Nedeljkovic JM (1993) Langmuir 9:980
18. Maxwell Garnett JC (1904) Phil Trans Royal Soc London 203:385
19. Jellinek HHT (1955) Degradation of Vinyl Polymers. Academic Press, New York, p 74
20. McNeill IC (1968) Eur Polym J 4:21
21. Marning LE (1988) Macromolecules 21:528
22. Kashiwagi T, Inaba A, Brown JE, Hatada K, Kitayama T, Masuda E (1986) Macromolecules 19:2160
23. Kashiwagi T, Hirata T, Brown JE (1985) Macromolecules 18:131
24. Hirata T, Kashiwagi T, Brown JE (1985) Macromolecules 18:1410
25. Marning LE, Sogah DY, Cohen GM (1989) Macromolecules 22:4652
26. Peterson JD, Vyazovkin S, Wight CA (1999) J Phys Chem B 103:8087
27. Ash BJ, Schadler LS, Siegel RW (2002) Mater Lett 55:83
28. Aymonier C, Bortzmeyer D, Thomann R, Mulhaupt R (2003) Chem Mater 15:4874
29. Sandeep K, Jyoti PJ, Upendra N (2003) J Appl Polym Sci 89:1186
30. Yang M, Dan Y (2005) Colloid Polym Sci 284:243
31. Gao Z, Xie W, Hwu JM, Wells L, Pan WP (2001) J Therm Anal Calorim 64:467
32. Hu YH, Chen CY, Wang CC (2004) Polym Degrad Stab 84:545